Self-focusing in chromium-doped potassium niobate single ceramic crystal

J. Castillo-Torres[a,*], J. Hernández A.[b,**], S. Gonzalez-Martínez[a],
A. Aguirre-López[a], M. B. Hernández[a], and J.A. Aguilar-Martínez[a]
[a]*Instituto de Física y Matematicas, Universidad Tecnológica de la Mixteca,*
069000, Huajuapan de León, Oaxaca, México,
[b]*Instituto de Física, Universidad Nacional Autónoma de México,*
PO Box 20-364, 01000 México, D.F., México,
e-mail: jaimec@mixteco.utm.mx, josemh@fisica.unam.mx***

Recibido el 23 de agosto de 2006; aceptado el 26 de octubre de 2006

The self-focusing and nonlinear optical absorption in a chromium-doped potassium niobate single ceramic crystal have been investigated. The third-order electric susceptibility $\chi^{(3)}$ at continuous 532 nm radiation is estimated based on a band transport model describing photorefractive properties for this electro-optic material. An anisotropic behavior on its nonlinear optical absorption properties has also been observed due to the presence of chromium ions.

Keywords: Self-focusing; nonlinear electric susceptibility.

Se investigó el auto-enfocamiento y la absorción óptica no lineal en un cristal cerámico de niobato de potasio dopado con cromo. Se estimó el valor de la susceptibilidad eléctrica a tercer orden $\chi^{(3)}$ para una radiación continua de 532 nm sobre la base de un modelo de transporte de banda que describe las propiedades fotorefractivas para este material electro-óptico. También se observó un comportamiento anisótropo en sus propiedades ópticas no lineales debido a la presencia de iones de cromo.

Descriptores: Auto-enfocamiento; susceptibilidad eléctrica no lineal.

PACS: 78.20.Ci; 77.84.Dy

1. Introduction

Much of the research done with photorefractive materials involves the writing of a holographic grating through the interference of two beams of light within the photorefractive material. Nevertheless, there has been some interest in the effects of arbitrary light beams on these materials. For instance, if one is interested in the propagation of light with no distortions through these media, *i.e.* soliton production, it is important to determine the spatial dependence of the refractive index as a result of the photorefractive interaction. Recently, there has also been interest in observing spatial solitons in photorefractive materials. The photorefractive spatial solitons which arise from the self-focusing effect have exceptionally low optical power in the microwatt range and can be achieved by using continuous-wave laser irradiance. Since the prediction of the photorefractive spatial solitons [1], they have been produced in $Sr_xBa_{1-x}Nb_2O_6$, $Bi_{12}TiO_{20}$, $Bi_{12}SiO_{20}$, $LiNbO_3$, and in InP [2]. In order to study theoretically and experimentally the photorefractive spatial solitons, an experimental characterization of the nonlinearities is necessary. The most suitable experimental tool for this purpose is perhaps the z-scan technique [3]. Here the optically nonlinear medium is illuminated by a focused laser beam, usually with a Gaussian profile; the information about the nonlinearities is obtained from the dependence of the far-field on-axis irradiance on the position of the sample relative to the focal point. In this work, both real and the imaginary parts of the third-order electric susceptibility for Cr:$KNbO_3$ are obtained. In addition, an anisotropic behavior in its optical absorption properties has been observed, *i.e.* a dependence on the incident light polarization orientation exists.

2. Theory

The z-scan technique is useful to measure the nonlinear refractive index and nonlinear absorption coefficient associated with the real $\chi^{(3)}_{Re}$ and imaginary $\chi^{(3)}_{Im}$ parts of the third-order electric susceptibility $\chi^{(3)}$ respectively, for nonlinear optical materials. After the introduction of this versatile technique, it became very popular mainly due to its simplicity and accuracy. This method basically consists in translating a nonlinear sample along the optical-axis in the focal region of an inhomogeneous-profile focused light beam, usually a single Gaussian TEM_{00} beam, for measuring simultaneously the transmitted light intensity by means of a photodetector in the far field region (see Fig. 1 below). The laser beam is focused with a lens in order to enhance the optically induced nonlinear response. If the medium exhibits purely intensity-induced refractive index changes, the light passed through an aperture placed in front of the photodetector (called the "closed aperture condition") is thus recorded as the sample is scanned around the focal point. On the other hand, if the material also shows nonlinear absorption arising from either direct multiphoton absorption, saturation of the single photon absorption, or dynamic free-carrier absorption, one can remove the aperture (known as the "open aperture condition") for detecting the intensity-induced absorption changes alone. In the presence of any nonlinear absorption in the closed aperture condition (or better, the "partially closed aperture condition"), the

nonlinear refractive index cannot be directly obtained from these experimental data. However, if one makes another scanning without the aperture and divides the closed aperture normalized z-scan data by that with the open aperture, a new z-scan is obtained which agrees to within 10% with that measured from a purely refractive z-scan. Bound electronic nonlinear refraction is the principal physical mechanism, $i.e.$ Kerr-type nonlinearity, which occurs in most nonlinear optical solids, although it is not the only one. For example, if the material has a photorefractive response, a non-local photo-induced charge displacement process has to be taken into account.

To that end, we consider the so-called "material equations" [4] of a photorefractive medium in steady state:

$$[s(I_0+I_d)+\beta_T]\,(N_D-N_D^+)-\gamma_R N N_D^+=0 \quad (1)$$

$$J=e\mu NE+\mu k_B T\frac{dN}{dx}+sC_p(N_D-N_D^+)(I_0+I_d) \quad (2)$$

$$\frac{dE}{dx}+\frac{e}{\epsilon\epsilon_0}(N+N_A-N_D^+)=0 \quad (3)$$

where s is the photoexcitation cross section, I_0 is the intensity of the focused laser beam, I_d is the so-called dark irradiance, β_T is the thermal excitation rate, N_D is the volume density of total donors, N_D^+ is the density of ionized donors (acceptors), N_A is the density of non-photoactive ions (that compensate the ionized donors N_D^+ in the dark), N is the density of photo-induced charge carried in the conduction or valence band, γ_R is the recombination coefficient, J is the electric current density, e is the positive or negative elemental charge, μ is the charge mobility, E is the space-charge field, k_B is the Boltzmann constant, T is the absolute temperature, C_p is the photovoltaic constant for the polarization used in this configuration, ϵ is the dielectric permittivity of the crystal, and ϵ_0 is the permittivity of free space.

In typical photorefractive materials, N_D, N_D^+, $N_A \gg N$ can be assumed for cw laser irradiance. Resolving Eqs. (1),(2) and (3), we obtain the refractive index perturbation

$$\Delta n=\Delta n_1\frac{I_0}{I_0+I_d} \quad (4)$$

where $\Delta n_1=(1/2)n_0^3 rE$ is the saturable refractive index perturbation, n_0 is the unperturbed background index of refraction, and r is the electro-optic coefficient. The following relations can be readily deduced for some nonlinear optical parameters in cgs and MKS units:

$$\gamma=80\pi(cn_0)^{-1}n_2\,,$$

$$\gamma=3(4\epsilon_0 cn_0^2)^{-1}\chi^{(3)}_{Re[MKS]}\,,$$

$$n_2{=}3\pi(2n_0)^{-1}\chi^{(3)}_{Re[esu]}$$

$$\chi^{(3)}_{Im[MKS]}{=}n_0^2\epsilon_0 c\lambda_0(2\pi)^{-1}\beta\,,$$

$$\chi^{(3)}_{Re[MKS]}=(160\pi^2\epsilon_0)\chi^{(3)}_{Re[esu]} \quad (5)$$

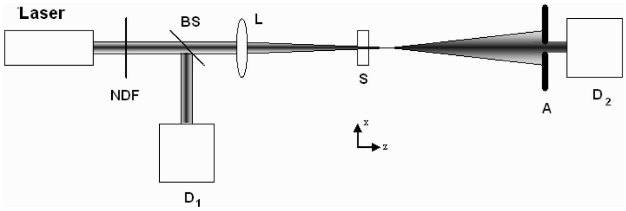

FIGURE 1. Experimental scheme for the z-scan technique. The $KNbO_3$:Cr sample is moved along the laser beam propagation axis. NDF is a neutral density filter. BS is a beam splitter. L is a convergence lens. S is the sample. A is an aperture. D_1, D_2 are input and output energy monitors, respectively.

where $\chi^{(3)}_{Re}$ and $\chi^{(3)}_{Im}$ are real and imaginary parts of third order nonlinear susceptibility, respectively. n_2 and α_2 are both nonlinear indexes in the cgs system related to γ and β by $n=n_0+n_2|E|^2=n_0+\gamma I_0$; $\alpha=\alpha_0+\alpha_2|E|^2=\alpha_0+\beta I_0$, α_0 is the linear absorption coefficient, c is the speed of light, and λ_0 the beam wavelength in a vacuum. Because we use a Gaussian laser beam with the TEM_{00} mode as the probe beam, the complex amplitude of the light can be written as:

$$\Psi(x,z){=}\Psi_0\sqrt{\frac{\omega_0}{\omega(z)}}\exp\left[-\frac{x^2}{\omega^2(z)}-\frac{ikx^2}{2R(z)}\right]\times\exp[-i\phi(z)] \quad (6)$$

where, $\omega^2(z){=}\omega_0^2(1+z^2/z_0^2)$, ω_0 is the beam waist, $z_0{=}k\omega_0^2/2$ is the confocal parameter of the beam, $R(z){=}z(1+z_0^2/z^2)$ is the radius of curvature of the wavefront at z, $k=2\pi/\lambda_0$ is the wave number, and Ψ_0 is the wave amplitude at the focus. Inserting the intensity $I(x,z){=}|\Psi(x,z)|^2$ from Eq.(6) into Eq.(4) and expanding the exponential function, we get

$$\Delta n(x,z)=\frac{\xi(z)\Delta n_0}{1+\xi(z)}-\frac{2\xi(z)\Delta n_0 x^2}{\omega^2(z)\,[1+\xi(z)]^2} \quad (7)$$

where

$$\xi(z)=\frac{I(0,z)}{I_d}=\frac{I_0}{I_d}\frac{\omega_0}{\omega(z)}=\frac{\xi_0}{\left[1+\frac{z^2}{z_0^2}\right]^{1/2}} \quad (8)$$

$\xi_0=I_0/I_d$ being the intensity ratio of the focused beam at the waist. Now, if we assume a thin sample to neglect the change in beam size within the crystal due to either diffraction or refraction, that is, $n_0 z_0 \gg L$ where L is the sample thickness in the direction of beam propagation, the phase change of the beam through the crystal is:

$$\Delta\phi(x,z)=-\frac{k\xi_0\Delta\phi_0 x^2}{z_0\sqrt{1+\frac{z^2}{z_0^2}}\left(\sqrt{1+\frac{z^2}{z_0^2}}+\xi_0\right)} \quad (9)$$

where $\Delta\phi_0=k\Delta n_0 L$. In this way, the complex amplitude of the Gaussian beam exiting the sample in the far field, when

including the initial beam curvature of the focused beam, is given by

$$\Psi(x,z,\Delta\phi_0) = \Psi_1(0,z)\sqrt{\tfrac{\Omega_0(z)}{\Omega(z)}}\exp(-\alpha_0 L/2) \times\exp\left[-\tfrac{x^2}{\Omega^2(z)} - \tfrac{ikx^2}{2R_d} + i\theta\right] \quad (10)$$

where d is defined as the far field distance in free space, and the other parameters are expressed as:

$$\Psi_1(0,z) = \frac{\Psi_0}{\left(1+\frac{z^2}{z_0^2}\right)^{1/4}}$$

$$\Omega^2(z) = \Omega_0^2(z)\left[g^2(\Delta\phi_0) + \frac{d^2}{d_0^2}\right]$$

$$R_d = d\left[1 - \frac{g(\Delta\phi_0)}{g^2(\Delta\phi_0)+\frac{d^2}{d_0^2}}\right]^{-1}$$

$$\theta = \frac{1}{2}\arctan\left[\frac{z}{z_0}\right] + \frac{\xi(z)}{1+\xi(z)}\Delta\phi_0 + \frac{1}{2}\arctan\left[\frac{d/d_0}{g(\Delta\phi_0)}\right]$$

$$\Omega_0^2(z) = \omega_0^2\left[1+\frac{z^2}{z_0^2}\right], d_0 = \frac{1}{2}k\Omega_0^2$$

$$g(\Delta\phi_0) = 1 + \frac{d}{R_c}$$

$$\frac{1}{R_c(z)} = \frac{1}{R(z)} + \frac{2\xi_0\Delta\phi_0}{z_0\sqrt{1+\frac{z^2}{z_0^2}}\left[\sqrt{1+\frac{z^2}{z_0^2}}+\xi_0\right]^2}.$$

Finally, if we define $Z = z/z_0$ and $Z_1 = \sqrt{1+Z^2}$, the normalized z-scan transmittance at the on-axis position (x=0) with aperture can then be written as:

$$T(Z,\Delta\phi_0) = \frac{Z_1\left(Z_1+\xi_0\right)^2}{\sqrt{\left[Z_1\left(Z_1+\xi_0\right)^2 + 2\xi_0\Delta\phi_0 Z\right]^2 + 4\xi_0^2\Delta\phi_0^2}}. \quad (11)$$

On the other hand, the normalized beam transmittance with no aperture is given by:

$$T = 1 - \frac{q_0}{2\sqrt{2}}, \text{ being } q_0 = I_0 L_{eff}\beta\left[1+Z^2\right]^{-1} \quad (12)$$

where $L_{eff} = (1-e^{-L\alpha_0})/\alpha_0$ is the effective propagation distance within the material over which an optical nonlinear change is induced. An alternative way for obtaining the nonlinear refractive index is by means of [3]

$$\Delta T_{p-v} = 0.406(1-S)^{1/4}|\Delta\Theta_0| \quad (13)$$

$$\Delta Z_{p-v} = (1.717)z_0 \quad (14)$$

Where ΔT_{p-v} and ΔZ_{p-v} represent the peak-valley distances of the experimental curve on the ordinate and abscissa-axis, respectively, and S is the aperture size which can be appropriately defined as a ratio of the powers on the detector with and without aperture, and $\Delta\Theta_0 = 2\pi L_{eff}\gamma I_0/\lambda_0$.

3. Results and Discussion

The z-scan setup is depicted in Fig. 1, in which the crystallographic c-axis of our $KNbO_3$:Cr crystal (1.01 mm thickness) is initially oriented perpendicular to the beam polarization, as will be discussed below. Potassium niobate is orthorhombic (point group $mm2$) with the crystallographic b-axis in the pseudocubic [010] direction, while the a- and c-axes lie along the pseudocubic [101] and [101] directions. The sample dimensions ($a \times b \times c$) are 6.21mm × 1.01mm × 7.66mm, and it was grown by the Czochralski method (K_2O, 52.5 mol% and Nb_2O_5, 47.5 mol%) [5]. A concentration of 4000 ppm of chromium oxide (Cr_2O_3) was added into the melt, and a platinum crucible was used. The final product was in an as-grown state. The light source was an Nd^{3+}:YVO_4 laser operating at 532 nm with a minimum coherent length of about 10 cm. A Newport powermeter-835 with a silicon ultraviolet photodetector-818UV and a Melles-Griot powermeter 13-PEM 001/J were used. The laser beam was focused with an 11-cm focal length lens yielding a minimum waist radius of 23 μm (half-width at $1/e^2$ intensity maximum), and therefore 3.1 mm as confocal parameter is calculated. With the help of neutral density filters, we controlled the incident laser power upon the crystal.

By using a Perkin-Elmer spectrophotometer at room temperature, the linear absorption coefficient at 532 nm is obtained (see Fig. 2) and by means of a Two-Oscillator Sellmeier model the linear refractive index along the b-axis for our crystal was also calculated, which at 532 nm is n = 2.38. This figure also shows the difference in the optical absorption coefficient when the crystallographic c-axis (the optical axis) of the $KNbO_3$:Cr sample is parallel and when it is perpendicular to the beam polarization. The optical absorption spectrum does not show electronic transitions related to chromium ions. One possible explanation is that the chromium impurities were incorporated as aggregates into the host [6]. This means that impurities most probably entered the crystal lattice as chromium-oxide and not as divalent or trivalent interstitial chromium ions, thus increasing the absorption coefficient near the absorption edge region, between 400-500 nm, as is observed in Fig. 2. Experiments using Electron Paramagnetic Resonance and X-ray diffraction are under way to clarify the chromium valence state. In addition, we note that in the same Fig. 2, the linear absorption coefficient clearly depends on the incident-light polarization, $i.e.$ the sample exhibits linear dichroism in the visible range.

The normalized transmittance as a function of the crystal position in the open aperture condition is plotted in Fig. 3. The incident maximum irradiance was 2.6 KW/cm^2, where the expression $I = 2P/\pi\omega_0^2$ is used. By fitting Eq. (12) to these experimental data, we obtained 1.7 mm as the Rayleigh range of the focused beam and thus 17 μm as the minimum beam waist radius inside the crystal. In addition, $\beta = -16.7\mu m/W$ and $\chi_{Im}^{(3)} = -2.13\times10^{-14}m^2/V^2$ are

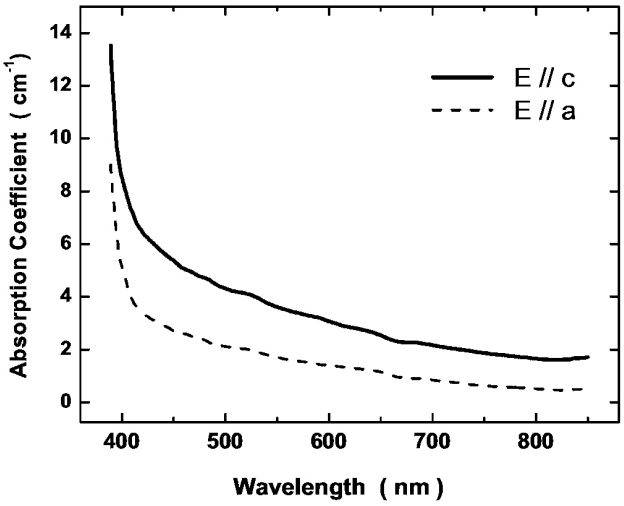

FIGURE 2. Absorption spectra of $KNbO_3$ crystal doped with 4000 ppm chromium oxide nominal concentration. Spectra were obtained with light polarization parallel (solid curve) and perpendicular (dashed curve) to the optical c-axis.

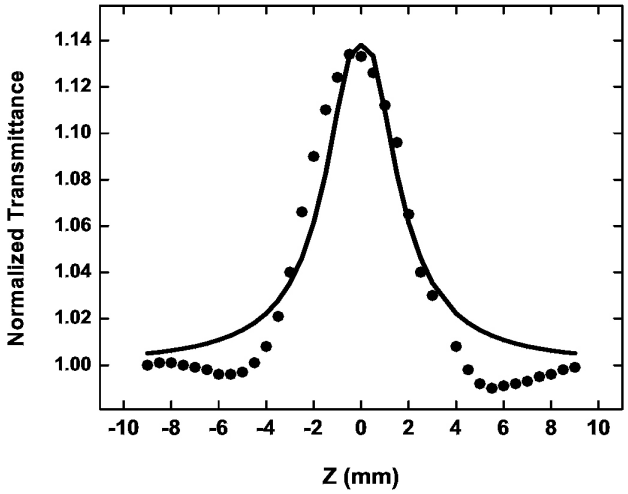

FIGURE 3. Z-scan open aperture normalized transmittance at 532 nm. The solid line is a fitting using Eq.(12).

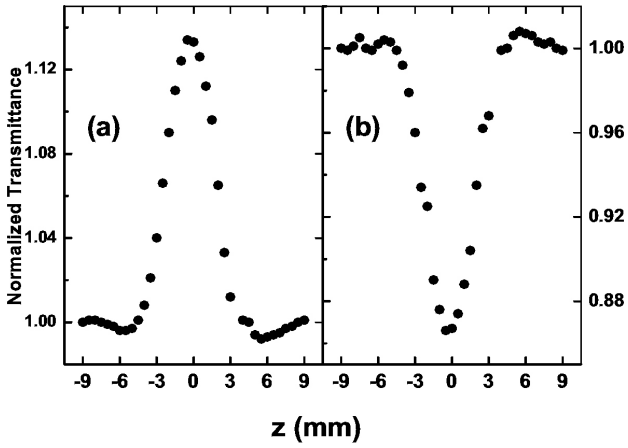

FIGURE 4. Transmittance with no aperture for two-crystallographic directions of the sample with respect to the laser beam electric field. (a) E $\perp$ c-axis. (b) E $\parallel$ c-axis.

also obtained. That is, either the increase of the transmission with power density or the negative sign of the values indicates that the sample shows a bleaching-like behavior (saturation of absorption) when its optical-axis is perpendicular to the beam polarization. Here the absolute error is around 8%, due mainly to variations in laser intensity.

On the other hand, if the crystallographic c-axis is parallel to the light polarization this material undergoes two-photon absorption; in Fig. 4, both cases for comparison are shown. In fact, these noticeable dependencies on radiation polarization, namely linear and nonlinear optical absorption (Figs. 2 and 4), were taken into account for an adequate explanation of the photorefractive response for this electro-optical material [7], and it is attributed to the presence of chromium ions. This anisotropic behavior could not be observed, or at least it has not been reported, in the $KNbO_3$:Fe crystal [8].

Besides absorption properties, the optically induced refractive index change is also obtained. The normalized transmittance as a function of the sample position in the closed aperture condition is measured, from which one can infer the refractive nonlinearity. In order to minimize substantially our systematic error due to the likely poor surface quality, a subtracting of the low irradiance background from the high irradiance z-scan after normalizing each datum is performed [3], as depicted in Fig. 5. Due to the formation of a photorefractive space-charge field and possible thermal effects [9], each plotted experimental data point corresponds to an average of ten independent measurements to compensate for temporal fluctuations. We chose at least two minutes before collecting one single data, and after illuminating the sample completely; this time is enough to erase any residual diffraction grating. In this host, the photorefractive erasure time typically ranges from $1ms$-$3s$ in the presence of a homogeneous light beam. For these measurements, the aperture size was $S = 0.1$

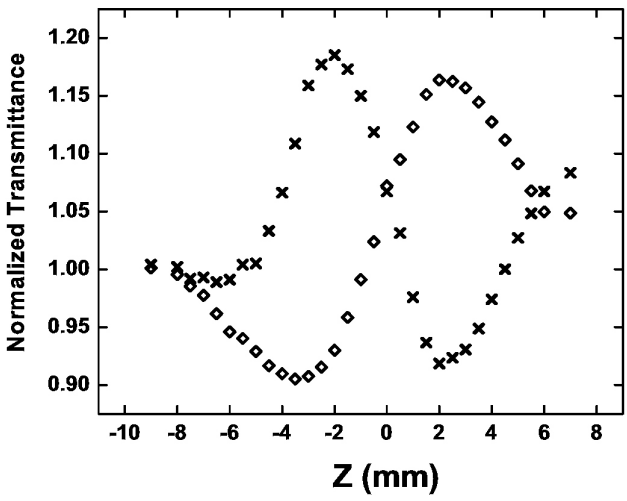

FIGURE 5. Normalized transmittance with an aperture of S =0.1 for low irradiance at $0.1 KW/cm^2$(crosses) and high irradiance at 1 KW/cm^2(diamonds).

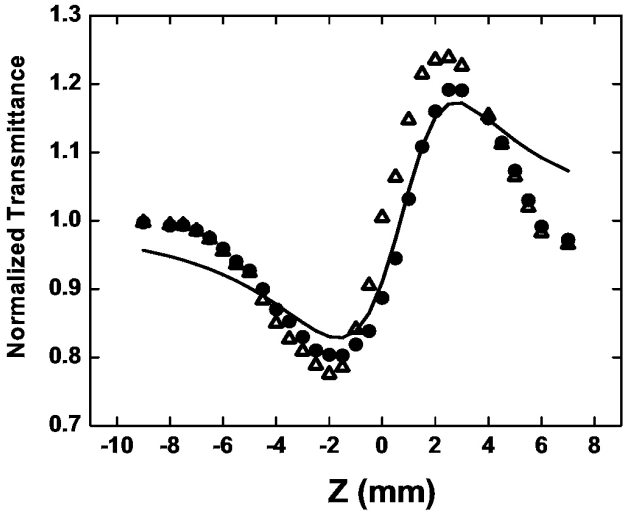

FIGURE 6. Net normalized transmittance after the background subtraction of the data in Fig. 5 (open triangles), after division by open aperture data from Fig. 3 (fullcircles), and the best fit with Eq. (11) to the full circle data(solid line).

allowing 10% linear transmittance, and the overall accuracy for each datum as well as for the final results is around 20%, mainly because of the fitting procedure. In materials showing strong linear absorption a temperature-dependent refractive index can be induced [10]. Although our sample not exhibit large linear absorption in 532 nm and consequently any thermal-lens effect may be considered negligible, we proceeded anyway to divide the closed aperture by the open aperture data to minimize the contributions of the nonlinear absorption response. Figure 6 shows this ratio along with the case not carrying out the division.

As can be seen from Fig. 6, there is almost no difference between these curves. Moreover, this similarity confirms what we deduced about the important absence of thermal effects. In addition, the shape of the curves in Fig. 6 shows, a valley followed by a peak transmittance which undoubtedly characterizes a positive nonlinear refractive index, *i.e.* a self-focusing of light beam inside the crystal is produced. A direct fitting of Eq. (11) with $\xi_0 \approx 1000$ and using Eq. (6), gives us a value of $\gamma = 11.6\text{pm}^2/\text{W}$ and thus $\chi^{(3)}_{Re} = 23.3\times10^{-14}\text{m}^2/\text{V}^2$. Again, $1.9mm$ as diffraction length and then $18\mu m$ as the minimum spot size inside the crystal are determined, both within the accuracy consistent with those obtained from the open aperture condition. In this case, as with many other ion-doped crystals [11] our sample suffers saturation nonlinearity. The saturable Kerr-type index perturbation in this single crystal occurs above 3KW/cm^2, as can be observed in Fig. 7, in which valley-peak vertical distance is plotted as a function of incident maximum power density. This saturation is due most probably to contributions of a higher-order nonlinear optical response.

Due to the positive nonlinear refractive index as shown from the closed aperture experiment in Fig. 6, the Gaussian minimum beam waist radius inside this material decreases, as expected. That is, it was found to become narrow with increasing intensity compared to the minimum spot size in air. On the other hand, the contrasting behavior between curves from Fig. 4 may be attributed to different signs in the third-order tensor susceptibilities elements, along the crystal orientations indicated. Certainly, instead of considering an absolute $\chi^{(3)}$, one should assign effective third-order susceptibility as a mean optical parameter related to their tensor elements, which depends on the material crystallographic structure and the direction of the incident wave vector $\mathbf{k}$. To our knowledge, pure-potassium niobate z-scan measurements have not yet been reported in the literature. However, we can make a comparison of the maximal refractive-index change between $KNbO_3$:Cr and $KNbO_3$:Fe. To that end, we use the following expression [12]:

$$\Delta n_1 = \left(\frac{\lambda_0}{L}\right)\left(\frac{\Delta\Theta_0}{2\pi}\right).$$

Therefore, the maximal nonlinear refractive index change value for $KNbO_3$:Fe is 3.5×10^{-5} according to Ref. 8, and 4.0×10^{-5} according to Ref. 12; whereas 10.1×10^{-5} is obtained for our $KNbO_3$: Cr crystal. Moreover, in Refs. 8 and 12, a negative nonlinear refractive index has been observed, whilst a positive nonlinear refractivity is reported in this work, as may be seen in Fig. 6. An extension of this analysis with other impurities at different levels is therefore desirable.

It is worth mentioning that Eqs. (11) and (12) have been derived using a beam complex amplitude, taking into account only one coordinate in its transversal section, as can be observed in Eq. (6). This is the explanation why the fittings in Fig. 3 and 6 are not so good, principally in the lateral-sides, except in the central regions, because the beam waist size is relatively unchanged. Despite this fact, we have developed and applied a first approximation to compare some nonlinear optical features between these two materials, *i.e.* chromium and iron-doped potassium niobate crystals.

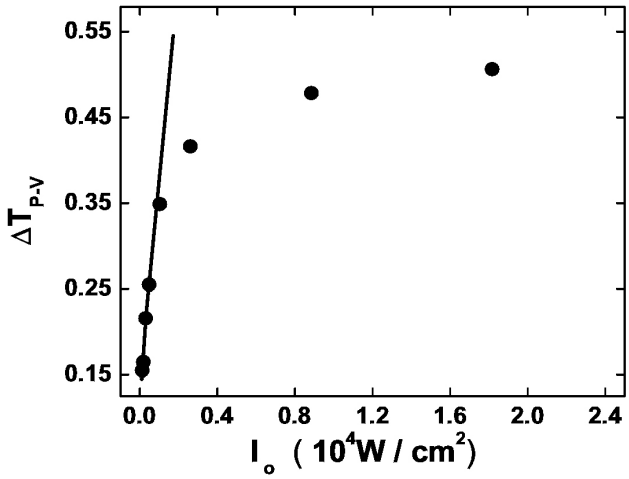

FIGURE 7. The peak-to-valley transmittance difference as a function of incident intensity at focus. Equation (13) describes the linear dependence at low intensities.

4. Conclusions

In summary, the sign and the magnitude of the real and imaginary parts of the third order nonlinearities $\chi^{(3)}$ for $KNbO_3$:Cr have been obtained at cw 532 nm. A band transport photorefractive model for the cross-section of a one-dimensional beam transversal section was employed for this purpose. This electro-optical system shows a strong dependence on the incident beam's polarization direction, not only for linear absorption but also for absorptive nonlinearities; it is therefore suggested that it can be used as a nonlinear optical switch. Unlike iron-doped potassium niobate, we have also found a positive sign associated with the nonlinear index refraction by means of z-scan measurements. Moreover, the maximum refractive-index change is higher for $KNbO_3$:Cr than for $KNbO_3$:Fe by almost one order of magnitude. Additional experiments are underway to clarify the chromium distribution state in the lattice of potassium niobate single crystal.

Acknowledgements

J. Castillo-Torres acknowledges with gratitude the financial support by Grant CONACYT (México) No. 46833. The authors also wish to thank Dr. C. Medrano for the crystals samples supplied.

1. M. Segev, B. Crosignani, A. Yariv, and B. Fisher, *Phys. Rev. Lett.* **68** (1992) 923.
2. W. Królikowski, B. Luther-Davies, and C. Denz, *IEEE J. Quantum Electron.* **39** (2003) 3.
3. M. Sheik-Bahae, A.A. Said, T.H. Wei, D.J. Hagan, and E.W.V. Stryland, *IEEE J. Quantum Electron.* **26** (1990) 760.
4. N.V. Kukhtarev, V.B. Markov, S.G. Odulov, M.S. Soskin, and V.L. Vinetskii, *Ferroelectrics* **22** (1979) 949.
5. W. Xing, H. Looser, H. Wüest, and H. Arend, *J. Cryst. Growth* **78** (1986) 431.
6. F. Agulló-López, C.R.A. Catlow, and P.D. Townsend, *Point Defects in Materials* (Academic Press, London,1988) p. 119.
7. J. Castillo-Torres, J. Hernández A., C. Medrano P., E. Camarillo G., and H. Murrieta S., *Opt. Mat.* **22** (2003) 251.
8. S.Q. Wang Song, Ch.P. Zhang, and P.J. Talbot, *Opt. Commun.* **98** (1993) 269.
9. P. Xie, I. Taj, and T. Mishima, *J. Opt. Soc. Am. B* **18** (2001) 479.
10. R. de Nalda *et al.*, *J. Opt. Soc. Am. B* **19** (2002) 289.
11. H.P. Li, C.H. Kam, Y.L. Lam and W. Ji, *Opt. Mat.* **15** (2001) 237.
12. R. Ryf, A. Lötscher, C. Bosshard, M. Zgonik, and P. Günter, *J. Opt. Soc. Am. B* **15** (1998) 989.